

## Unsteady Flow with Cavitation in Viscoelastic Pipes

Alexandre K. Soares<sup>1</sup>, Dídía I.C. Covas<sup>2</sup>, Helena M. Ramos<sup>2</sup> and Luisa Fernanda R. Reis<sup>3</sup>

<sup>1</sup>Department of Sanitary and Environmental Engineering, Federal University of Mato Grosso  
Ave. Fernando Correa da Costa, Cuiabá, 78060-900, Brazil, aksoares@ufmt.br

<sup>2</sup>Instituto Superior Técnico, Technical University of Lisbon (TULisbon)  
Ave. Rovisco Pais, Lisbon, 1049-001, Portugal, didia.covas@civil.ist.utl.pt, hr@civil.ist.utl.pt

<sup>3</sup>São Carlos School of Engineering, University of São Paulo  
Ave. Trabalhador São-carlense 400, São Carlos, 13566-590, Brazil, fernanda@sc.usp.br

### Abstract

The current paper focuses on the analysis of transient cavitating flow in pressurised polyethylene pipes, which are characterized by viscoelastic rheological behaviour. A hydraulic transient solver that describes fluid transients in plastic pipes has been developed. This solver incorporates the description of dynamic effects related to the energy dissipation (unsteady friction), the rheological mechanical behaviour of the viscoelastic pipe and the cavitating pipe flow. The Discrete Vapour Cavity Model (DVCM) and the Discrete Gas Cavity Model (DGCM) have been used to describe transient cavitating flow. Such models assume that discrete air cavities are formed in fixed sections of the pipeline and consider a constant wave speed in pipe reaches between these cavities. The cavity dimension (and pressure) is allowed to grow and collapse according to the mass conservation principle. An extensive experimental programme has been carried out in an experimental set-up composed of high-density polyethylene (HDPE) pipes, assembled at Instituto Superior Técnico of Lisbon, Portugal. The experimental facility is composed of a single pipeline with a total length of 203 m and inner diameter of 44 mm. The creep function of HDPE pipes was determined by using an inverse model based on transient pressure data collected during experimental runs without cavitating flow. Transient tests were carried out by the fast closure of the ball valves located at downstream end of the pipeline for the non-cavitating flow and at upstream for the cavitating flow. Once the rheological behaviour of HDPE pipes were known, computational simulations have been run in order to describe the hydraulic behaviour of the system for the cavitating pipe flow. The calibrated transient solver is capable of accurately describing the attenuation, dispersion and shape of observed transient pressures. The effects related to the viscoelasticity of HDPE pipes and to the occurrence of vapour pressures during the transient event are discussed.

**Keywords:** Cavitating flow, Fluid transients, Viscoelasticity, Pipelines, Experimental data.

### 1. Introduction

Typically, hydraulic transient analysis is carried out in the design of pressurised pipe systems in order to guarantee their security, reliability and good performance for various normal operating conditions [1-3]. This analysis is equally important in the operation stage for the diagnosis of existing problems and the calculation of different operational scenarios. Prediction of maximum transient pressures is used for the verification if pipe materials, pressure classes and wall-thicknesses are sufficient to withstand predicted pressure loads to avoid pipe rupture or system damage. Verification of minimum allowable pressures is important to prevent air release, cavitation and water column separation, and, consequently, avoid pipe collapse or pathogenic intrusion into the system. When severe transients cannot be avoided, either pipe layout and system parameters are changed (e.g., operating conditions), or surge protection devices are specified (e.g., pressurised vessels or air-relief valves), so as to sustain extreme transient pressures within acceptable limits. Usually, the decision is the most economical and reliable solution that yields an acceptable transient pressure response.

Classic water hammer theory is generally used, as it reasonably well describes extreme transient pressures. Most software packages available are based on this theory. The classic approach assumes that the pipe-wall has a linear-elastic rheological behaviour, friction losses are described by quasi-steady formulae, flow is one-phase and the pipe is completely constrained axially [2]. These assumptions are not always valid, as there are natural phenomena that rapidly attenuate or increase transient pressures

such as fluid friction during fast-transients [4], leaks [5], the mechanical behaviour of plastic pipes [6-8], dissolved or entrapped air [9-11] and multi-pipe systems.

The aim of the current paper is to present the results of the combination of different dynamic effects (i.e., pipe-wall viscoelasticity and cavitation) in hydraulic transient calculations as well as to discuss the importance of these phenomena in the analysis of each particular situation. For this purpose, physical data were collected from an experimental polyethylene (PE) pipeline, assembled in the Hydraulic Laboratory of Civil Engineering Department of Instituto Superior Técnico (Lisbon, Portugal). A series of transient tests were carried out collecting pressure at four different locations. A hydraulic transient solver incorporating the description of different phenomena (e.g., unsteady friction, pipe-wall viscoelasticity, distributed cavitation) has been developed and used to analyse these case studies. An inverse transient solver has been used to calibrate several parameters. Collected data are compared with the results of numerical simulations. Conclusions are drawn concerning the importance of considering these effects in design and during the system operation.

## 2. Mathematical Models

### 2.1 Viscoelastic model

Equations that describe the one-dimensional transient-state flows in viscoelastic closed conduits are the momentum and continuity equations (eqs. 1 and 2, respectively). Since the flow velocity and pressure (dependent variables) in transient flows are functions of time and space (independent variables), these equations are a set of two hyperbolic partial differential equations [1-3, 7]:

$$\frac{1}{A} \frac{dQ}{dt} + g \frac{\partial H}{\partial x} + gh_f = 0 \quad (1)$$

$$\frac{dH}{dt} + \frac{a_0^2}{gA} \frac{\partial Q}{\partial x} + \frac{2a_0^2}{g} \frac{d\varepsilon_r}{dt} = 0 \quad (2)$$

where  $x$  = coordinate along the pipe axis;  $t$  = time;  $H$  = piezometric head;  $Q$  = flow rate;  $a_0$  = celerity or elastic wave speed (dependent on the fluid compressibility, and on the physical properties and external constraints of the pipe);  $g$  = gravity acceleration;  $A$  = pipe cross-sectional area;  $\varepsilon_r$  = retarded strain component (in viscoelastic pipes the total strain can be decomposed into an instantaneous-elastic strain and a retarded strain); and  $h_f$  = head loss per unit length ( $h_f = fQ|Q|/2DA^2$  in turbulent conditions, in which  $f$  = Darcy-Weisbach friction factor and  $D$  = pipe inner diameter). These equations assume: pseudo-uniform velocity profile; linear viscoelastic rheological behaviour of the pipe-wall; one-phase, homogenous and compressible fluid, though with negligible changes in density and temperature; uniform and completely constrained from axial or lateral movement pipe.

The set of differential equations (eqs. 1 and 2) can be solved by the Method of Characteristics (MOC). The stability of this method requires the verification of a numerical restriction for the time and space steps, given by the Courant-Friedrich-Lewy stability condition,  $dx/dt = V \pm a_0$ . This condition allows the transformation of these equations into a set of total differential equations valid along the characteristic lines  $dx/dt = \pm a_0$ :

$$C^\pm : \frac{dH}{dt} \pm \frac{a_0}{gA} \frac{dQ}{dt} \pm a_0 h_f + \frac{2a_0^2}{g} \left( \frac{\partial \varepsilon_r}{\partial t} \right) = 0 \quad (3)$$

The set of differential equations (eqs. 1 and 2) together with the strain-stress equation (eq. 4) can be solved by the Method of Characteristics. The total strain generated by a continuous application of a stress  $\sigma(t)$  is:

$$\varepsilon(t) = J_0 \sigma(t) + \int_0^t \sigma(t-t') \frac{\partial J(t')}{\partial t'} dt' \quad (4)$$

in which  $J_0$  is the instantaneous creep compliance and  $J(t')$  the creep function at  $t'$  time.

In these equations, the retarded strain time-derivative term cannot be directly calculated and requires further numerical discretization. In order to numerically describe the rheological mechanical behaviour of the pipe-walls (creep function), the generalized Kelvin-Voigt mechanical model of a viscoelastic solid is incorporated in the hydraulic transient equations [12]:

$$J(t) = J_0 + \sum_{k=1}^{N_{KV}} J_k \left( 1 - e^{-t/\tau_k} \right) \quad (5)$$

where  $J_0$  = creep compliance of the first spring defined by  $J_0 = 1/E_0$ ;  $E_0$  = Young's modulus of elasticity of the pipe;  $J_k$  = creep compliance of the spring of the Kelvin-Voigt  $k$ -element defined by  $J_k = 1/E_k$ ;  $E_k$  = modulus of elasticity of the spring of  $k$ -element;  $\tau_k$  = retardation time of the dashpot of  $k$ -element,  $\tau_k = \mu_k/E_k$ ;  $\mu_k$  = viscosity of the dashpot of  $k$ -element; and  $N_{KV}$  = number of Kelvin-Voigt elements. Parameters  $J_k$  and  $\tau_k$  are determined by inverse calculation from experimental data. According to this mathematical model, the terms  $\partial \varepsilon_r / \partial t$  and  $\varepsilon_r$  are calculated as the sum of these factors for each Kelvin-Voigt element  $k$ :

$$\frac{\partial \varepsilon_r(i,t)}{\partial t} = \sum_{k=1}^{N_{KV}} \frac{\partial \varepsilon_{rk}(i,t)}{\partial t} = \sum_{k=1}^{N_{KV}} \left\{ \frac{\alpha D \gamma}{2e} \frac{J_k}{\tau_k} [H(i,t) - H_0(i)] - \frac{\varepsilon_{rk}(i,t)}{\tau_k} \right\} \quad (6)$$

$$\varepsilon_r(i,t) = \sum_{k=1}^{N_{KV}} \varepsilon_{rk}(i,t) = \sum_{k=1}^{N_{KV}} \left[ J_k F(i,t) - J_k e^{-\frac{\Delta t}{\tau_k}} F(i,t - \Delta t) - J_k \tau_k (1 - e^{-\frac{\Delta t}{\tau_k}}) \frac{F(i,t) - F(i,t - \Delta t)}{\Delta t} + e^{-\frac{\Delta t}{\tau_k}} \varepsilon_{rk}(i,t - \Delta t) \right] \quad (7)$$

where the function  $F(i,t)$  is defined by:

$$F(i,t) = \frac{\alpha D \gamma}{2e} [H(i,t) - H_0(i)] \quad (8)$$

where  $\gamma$  = fluid volumetric weight;  $e$  = pipe-wall thickness; and  $\alpha$  = dimensionless parameter (function of pipe cross-section dimensions and constraints).

At any interior grid intersection point, the two compatibility equations (eq. 3) and eqs. 6 and 7 are solved simultaneously for the unknowns  $\varepsilon_r(i,t)$ ,  $Q_{i,t}$  and  $H_{i,t}$ . In this research work, a general, simplified linear form for the linear-elastic conduit or the linear-viscoelastic pipe useful for complex, multi-pipe systems has been used [13]. To complete the solution at any time instant, appropriate boundary conditions have been introduced specifying additional equations at the ends of each pipe [1-3].

## 2.2 Discrete vapour cavity model (DVCM)

The discrete vapour cavity model (DVCM) is widely used in standard water hammer software packages for column separation and distributed cavitation analyses [14]. This model is based on the column separation hypothesis that the flow of liquid in the tube is instantaneously and completely separated by its vapour phase when the cavity is formed. Cavities are allowed to form at any of the computational sections if the pressure is computed to be below the vapour pressure. Pure liquid with a constant wave speed is assumed to occupy the reach in between two computational sections. The absolute pressure in a cavity is set equal to the vapour pressure ( $p^* = p_v^*$ ). The upstream and downstream discharges  $Q_{Pu}$  and  $Q_P$  at a cavity are computed from the compatibility relations (eq. 3), and, ignoring mass transfer during cavitation, its volume follows then from:

$$\frac{d\forall}{dt} = Q_P - Q_{Pu} \quad (9)$$

which is numerically approximated in the Method of Characteristics with a staggered grid by:

$$\forall_P^t = \forall_P^{t-2\Delta t} + \left[ \psi(Q_P^t - Q_{Pu}^t) + (1 - \psi)(Q_P^{t-2\Delta t} - Q_{Pu}^{t-2\Delta t}) \right] 2\Delta t \quad (10)$$

in which  $\forall_P^t$  and  $\forall_P^{t-2\Delta t}$  are the volumes at the current time and at  $2\Delta t$  earlier, and  $\psi$  is a numerical weighting factor. The cavity collapses when its calculated volume becomes less than zero. The liquid phase is re-established and the standard water hammer procedure is valid again.

Although the vapour column separation model is easily implemented, it has some serious deficiencies as stated by Shu [15]: (i) to avoid the prediction of negative cavity sizes (or the prediction of negative absolute pressures), artificial restrictions are imposed, which result in unrealistically large pressure spikes that discredit the overall value of the numerical results; (ii) the internal boundary condition permits vapour cavities to be formed only at computing nodes, and the simulation results are biased according to where the computing nodes are located; (iii) because the size of the cavity and its mass transfer are ignored, the model is clearly limited in its ability to model cavitation correctly; (iv) at each computing node, a flow rate discontinuity is assumed and there will be two predicted values of flow rate, which is clearly inconsistent with the observed behaviour at each point. In addition, the difference between the two predicted values increases when there is a high degree of cavitation and also when the number of computing nodes is small. On the other hand, when a large number of computing nodes is used, there are a corresponding number of discontinuities leading to a mathematical model that is ill defined. Simpson and Bergant [16] recommended that the maximum volume of discrete cavities at sections is less than 10% of the reach volume.

## 2.3 Discrete gas cavity model (DGCM)

Transient flow of a homogeneous gas-liquid mixture can be described by the classical water hammer equations in which the liquid wave speed  $a_0$  is replaced by the wave speed  $a_m$  [17]:

$$a_m = \frac{a_0}{\sqrt{1 + \frac{\alpha_g \rho a_0^2}{p^*}}} \quad (11)$$

where  $\alpha_g$  = gas void fraction; and  $\rho$  = liquid mass density.

An alternative to modelling free gas distributed throughout the liquid in a homogeneous mix can be achieved by lumping the mass of free gas at computing sections leading to the discrete gas cavity model (DGCM). Each isolated small volume of gas expands and contracts isothermally as the pressure varies, in accordance with the perfect gas law [2]:

$$(p^* - p_v^*)\forall = (p_0^* - p_v^*)\forall_0 = C_3 \quad (12)$$

An isothermal volume versus head relationship is assumed at a gas cavity:

$$\forall_P^t = \frac{C_3}{H_P^t - z - H_v} \quad (13)$$

in which the constant  $C_3$  can be computed from:

$$C_3 = \frac{p_0^* \alpha_0 \Delta x A}{\rho g} \quad (14)$$

where  $p_0^*$  = a reference absolute pressure;  $\alpha_0$  = void fraction at  $p_0$  (ratio of volume of free gas to the mixture volume);  $z$  = elevation of the pipe; and  $H_v$  = gauge vapour pressure head of the liquid.

As in the DVCM, between each computing section, and concentrated gas volume, pure liquid with a constant wave speed is assumed without free gas. The DGCM is also able to simulate vaporous cavitation by utilizing a low initial gas void fraction ( $\alpha_0 \leq 10^{-7}$ ) at all computational sections [16, 17].

## 2.4 Borga et al.'s model

Borga *et al.* [18] presented numerical results, which were obtained based on the traditional vapour-liquid model, introducing

several modifications in order to better simulate observed dissipation and dispersion of transient pressures due to mechanical, frictional and inertial dynamic effects. The following changes have been incorporated: (i) modification of Courant number; (ii) modification of friction loss coefficient (or head loss); (iii) modification of wave speed by an exponential law in time but uniform along the pipe axis; and (iv) modification of coefficients of the characteristic equations which affect the transformation of kinetic energy into elastic one and vice-versa.

The modification of the head loss coefficient is obtained by using a multiplicative coefficient,  $KR$ , and a coefficient of second order term in the integration of head loss,  $KT$ .

In the simulation of the variable celerity, it is considered an exponential variation along time, uniform along the entire pipe, according to the following equation:

$$a = a_0 \cdot a_f + a_0 (1 - a_f) e^{-\frac{t}{CT}} \quad (15)$$

where  $a_0$  and  $a_0 \cdot a_f$  = the wave speed values at initial and final time, respectively;  $CT$  = a parameter which affects the wave speed time variation. The wave speed variation was carried out at the same time by a time step variation  $\Delta t$ , in order to avoid Courant modification.

For the description of fluid and pipe material non-elastic behaviour, two reduction coefficients ( $KH$  and  $KQ$ ) were included in the MOC equations:

$$\Delta H = KH \frac{a}{gA} \Delta Q - I \quad (16)$$

$$\Delta Q = KQ \frac{\Delta H - I}{a / (gA)} \quad (17)$$

where  $I$  = the head loss term;  $\Delta H$  and  $\Delta Q$  = head and discharge variation, respectively.

Parameter  $KH$  gives a reduction in the head variation when induced by a discharge variation by non-elastic fluid (due to the presence of free gas) and pipe (plastics) deformation.  $KQ$  is a reduction coefficient in the discharge value caused by a head variation, due to a non-elastic response in the recuperation phase of the deformation.

### 3. Case Study

An extensive experimental programme has been carried out in an experimental set-up composed of high-density polyethylene (HDPE) pipes, assembled at Instituto Superior Técnico of Lisbon, Portugal (Fig. 1). The experimental facility is composed of a single transmission pipeline with a total length of 203 m and inner diameter of 44 mm. This pipeline is connected to an air vessel at the upstream end and to a free discharge outlet into a constant water level at the downstream end. A ball valve is installed immediately downstream the air vessel and it is used to interrupt the flow in order to perform a fast closing manoeuvre. The air vessel was used to keep the upstream pressure constant as an elevated reservoir. Transient pressure data have been collected using pressure transducers located at four pipe sections with a frequency of 500 Hz (at the air vessel; downstream the ball valve at upstream end of the pipeline - Section 1; at the middle of the pipeline - Section 5; and at downstream end of the pipeline - Section 6).

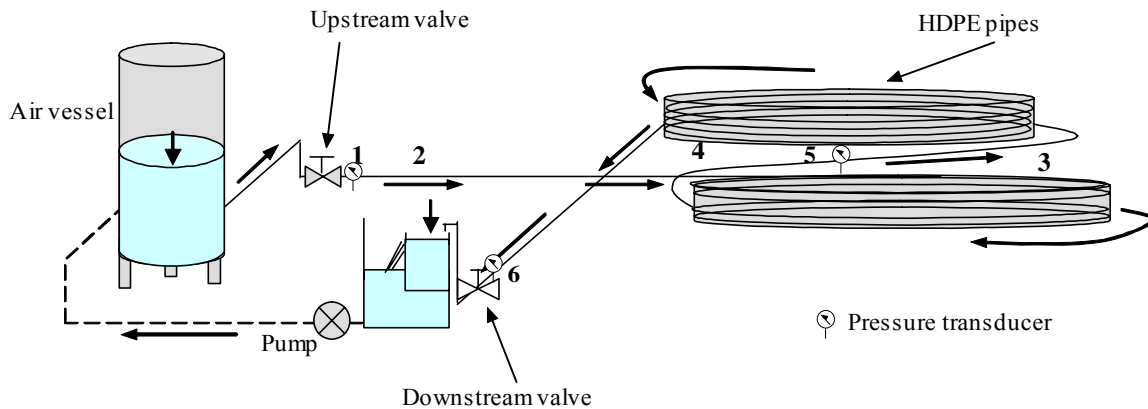


Fig. 1 Experimental set-up with high-density polyethylene pipes

### 4. Model Calibration

In order to analyze the pressure transients in the system, two different tests have been carried out: (i) fast closure of downstream end ball valve (without cavitating flow) for creep function analysis; and (ii) fast closure of the upstream end ball valve for cavitating flow analyses utilizing DVCM, DGCM and Borga *et al.*'s [18] model.

#### 4.1 Pipe-wall viscoelasticity analysis

In order to determine the mechanical behaviour of the HDPE pipe system, transient tests were carried out by closing the downstream end ball valve (without cavitation). The viscoelastic transient solver developed in this study was used neglecting unsteady friction and the HDPE creep function was numerically determined by means of inverse calculations.

The creep compliance function  $J(t)$  is numerically described by the generalized Kelvin-Voigt mechanical model. This model is

represented by the instantaneous elastic creep  $J_0$  and the retarded coefficients,  $J_k$  and  $\tau_k$  for each Kelvin-Voigt element. Usually this creep compliance function is unknown and it has to be experimentally estimated, either by using an inverse procedure (calibration) or by carrying out mechanical tensile tests of pipe specimens.

An inverse model based on Levenberg-Marquardt search method (LM) has been developed and was used to determine the coefficients of the creep compliance function  $J(t)$ . Elastic wave speed was estimated as 315 m/s ( $E_0 = 1.43$  GPa;  $J_0 = 0.70$  GPa<sup>-1</sup>;  $\Delta t = 0.002$  s; and  $\Delta x = 0.63$  m).

Several initial numerical simulations were run to find the best number of Kelvin-Voigt elements. The optimal number of Kelvin-Voigt elements was obtained by using three elements ( $\tau_1 = 0.018$  s;  $J_1 = 0.256$  GPa<sup>-1</sup>;  $\tau_2 = 0.50$  s;  $J_2 = 0.238$  GPa<sup>-1</sup>; and  $\tau_3 = 3.0$  s;  $J_3 = 0.290$  GPa<sup>-1</sup>). A complete calibration analysis of the HDPE pipe rig can be found in Carriço [19].

Numerical results obtained by using the linear viscoelastic transient solver are presented in Fig. 2 ( $Q_0 = 2.72$  L/s;  $Re \approx 80,000$ ) for the Section 6 of the pipe rig (downstream end of the pipeline and immediately upstream the ball valve). Numerical results fitted observed pressure data extremely well. Unsteady friction losses are assumed to be described by the creep function calibrated.

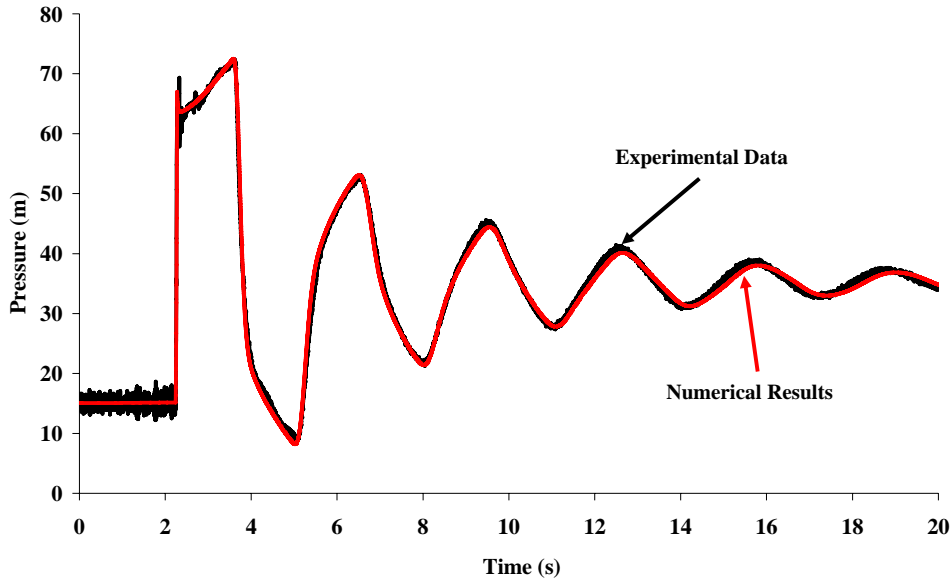


**Fig. 2** Numerical results (without cavitation and taking into account pipe-wall viscoelasticity) versus experimental data at Section 6 ( $Q_0 = 2.72$  L/s;  $Re \approx 80,000$ )

#### 4.2 Numerical results during cavitating flow

Transient tests were carried out by closing the upstream end ball valve to originate cavitating pipe flow in the system. Initially, the creep function calibrated for non-cavitation tests was used in order to describe the system mechanical behaviour. Actually, when pressure decreases and reaches the vapour pressure, a gas cavity is formed and consequently decreases the wave speed. In this way, a new set of viscoelastic parameters was determined and it has been assumed that unsteady friction losses, pipe-wall viscoelasticity and wave speed variation due to localised gas cavities were described by the creep function.

Elastic wave speed was estimated as 250 m/s ( $\Delta t = 0.08$  s and  $\Delta x = 20.0$  m) and three Kelvin-Voigt elements were used ( $\tau_1 = 0.10$  s;  $J_1 = 0.60$  GPa<sup>-1</sup>;  $\tau_2 = 0.50$  s;  $J_2 = 0.35$  GPa<sup>-1</sup>; and  $\tau_3 = 3.0$  s;  $J_3 = 0.50$  GPa<sup>-1</sup>).

The discrete vapour cavity model (DVCM) and the discrete gas cavity model (DGCM) developed in this study were used in order to describe the cavitating flow in the system. In the later, a small void fraction was adopted ( $\alpha_0 \leq 10^{-7}$ ), since the flow did not exhibit distributed air bubbles at the beginning of the tests.

Numerical results obtained by using the DVCM and the linear viscoelastic transient solver are presented for two locations of the pipe rig: Section 1 (upstream end of the pipeline and immediately downstream the ball valve – Fig. 3) and Section 5 (middle pipe section – Fig. 4).

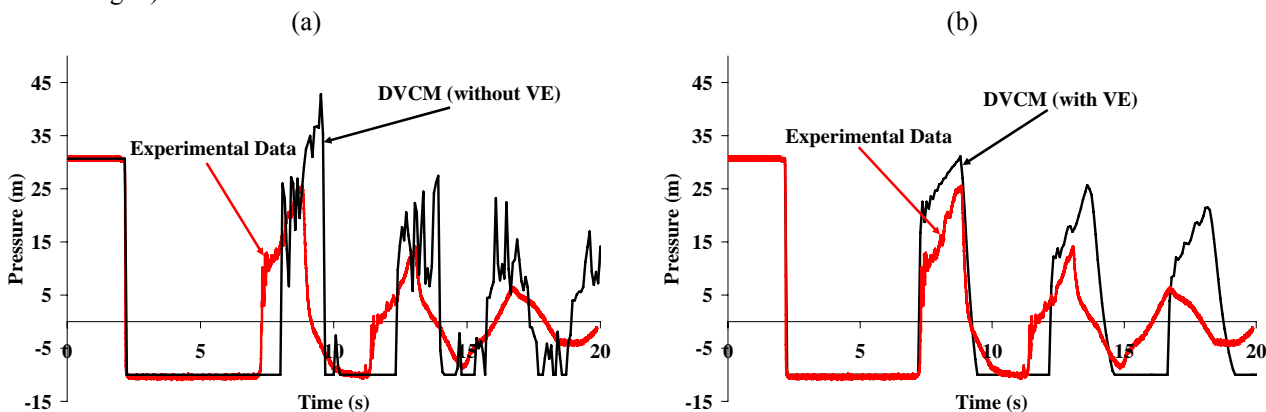


**Fig. 3** DVCM numerical results (a) neglecting and (b) taking into account pipe-wall viscoelasticity versus experimental data at Section 1 ( $Q_0 = 4.0$  L/s;  $Re \approx 120,000$ )

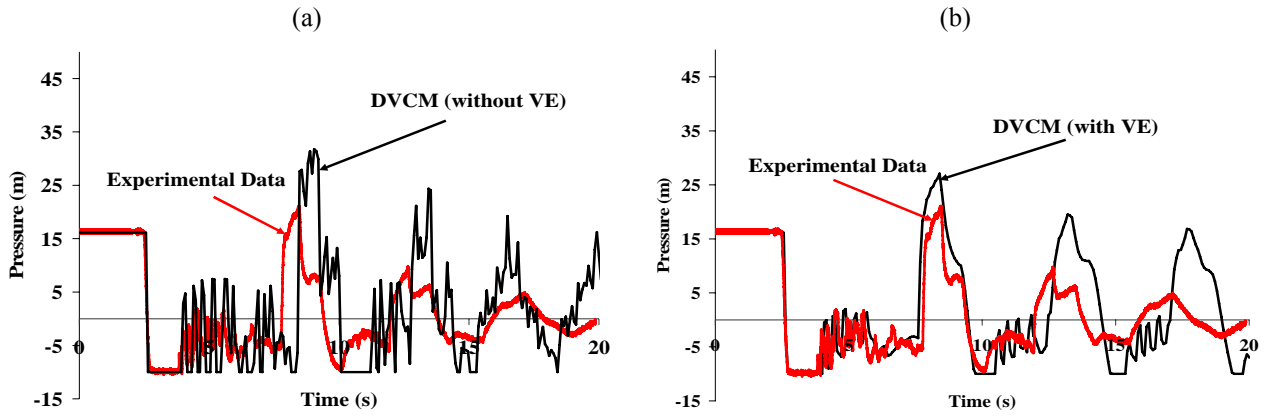


**Fig. 4** DVCM numerical results (a) neglecting and (b) taking into account pipe-wall viscoelasticity versus experimental data at Section 5 ( $Q_0 = 4.0$  L/s;  $Re \approx 120,000$ )

The use of DVCM taking into account pipe-wall viscoelasticity has shown that the attenuation and dispersion in the transient pressures were not described. In addition to the deficiencies pointed out by Shu [15], this is due to the assumption of the absolute pressure in the gas cavities being set equal to the vapour pressure and the energy dissipation during the expansion and contraction of the gas cavities being neglected.

In this way, the DGCM has been used in order to describe the system behaviour, considering a small initial void fraction ( $\alpha_0 \leq 10^{-7}$ ). Numerical results obtained by using the DGCM and the linear viscoelastic transient solver are presented for two locations of the pipe rig: Section 1 (upstream end of the pipeline and immediately downstream the ball valve – Fig. 5) and Section 5 (middle pipe section – Fig. 6).

The wave speed variation is shown in Fig. 7, considering the creep function determined. Starting from 250 m/s, the wave speed becomes nearly constant after 8.0 s with a final value of 167 m/s.

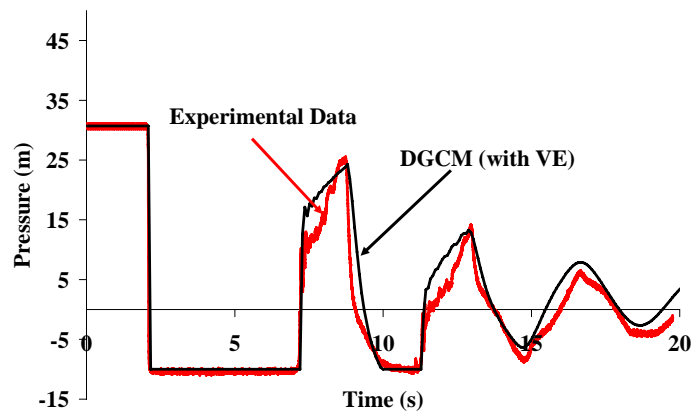


**Fig. 5** DGCM numerical results (taking into account pipe-wall viscoelasticity) versus experimental data at Section 1 ( $Q_0 = 4.0$  L/s;  $Re \approx 120,000$ )

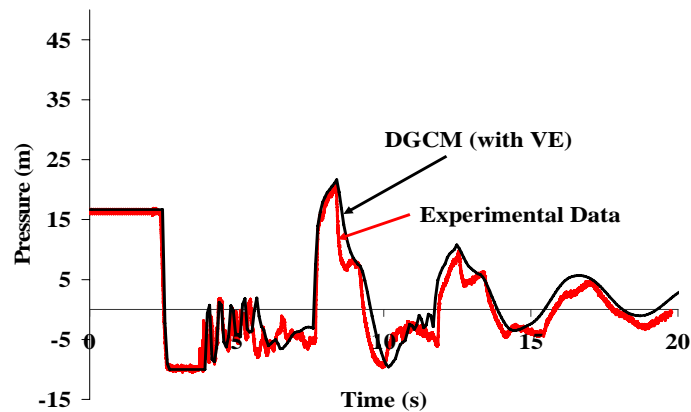


**Fig. 6** DGCM numerical results (taking into account pipe-wall viscoelasticity) versus experimental data at Section 5 ( $Q_0 = 4.0$  L/s;  $Re \approx 120,000$ )

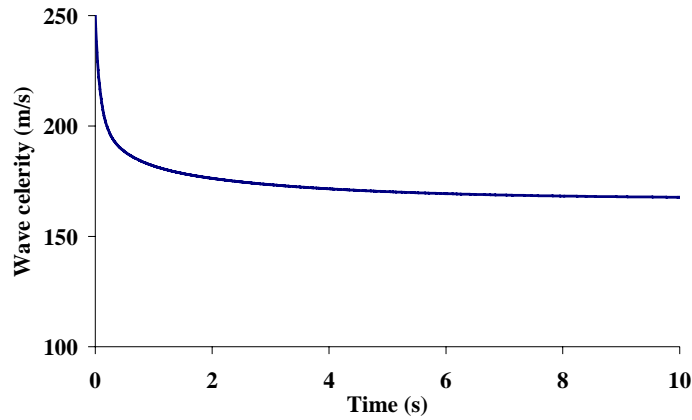


Fig. 7 Wave celerity variation

The use of DGCM taking into account pipe-wall viscoelasticity has shown that:

- (i) a better adjustment to the experimental data was obtained by DGCM than those one when utilizing the DVCM;
- (ii) the assumption of the ideal gas law is more appropriate than the simple adoption of vapour pressure when pressure reaches vapour pressure (DVCM) – this influences the energy dissipation during the expansion and contraction of gas cavities. In DGCM formulation, the exponent of the polytropic gas is assumed to be equal to 1.0 in order to obtain explicit equations and considering that the free gas is assumed to behave isothermally, which is valid for tiny bubbles. In this study, large bubbles were formed on the upper part of the pipe cross-section and growth along the pipe axis. Large bubbles and column separations tend to behave adiabatically. It is recommended further analyses of the exponent of the polytropic gas and of the implicit formulation;
- (iii) some features of the HDPE pipe rig during the transient tests, such as pipe displacement and a free discharge outlet at the downstream end of the pipeline, lead to more uncertainties on the system behaviour.

A third attempt in order to describe the system behaviour has been done by using Borga *et al.*'s [18] model. In this model, the authors have incorporated modifications in different characteristic parameters, such as wave celerity, head losses and coefficients of the characteristic equations. The numerical results were obtained by using the discrete vapour cavity model (DVCM).

Numerical results obtained by using Borga *et al.*'s model are depicted in Fig. 8 for transient pressures collected at Section 1, and in Fig. 9 for pressure variation at Section 5, considering the following parameters:  $a_0 = 300$  m/s;  $a_f = 0.8$ ;  $CT = 5$ ;  $KR = 1.0$ ;  $KT = 0.5$ ;  $KH = 0.4$ ; and  $KQ = 1.4$ .

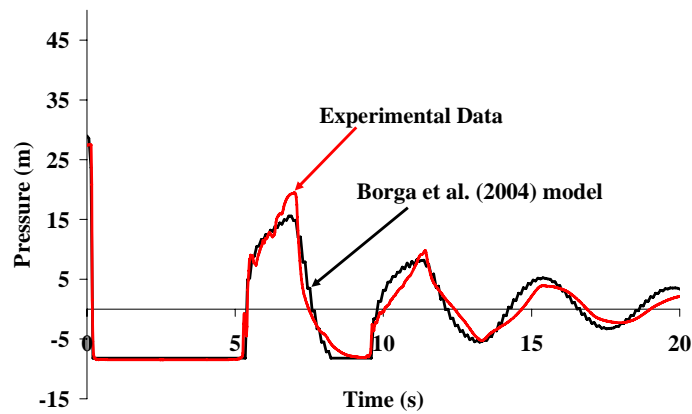


Fig. 8 Borga *et al.*'s model numerical results versus experimental data at Section 1 ( $Q_0 = 4.0$  L/s;  $Re \approx 120,000$ )

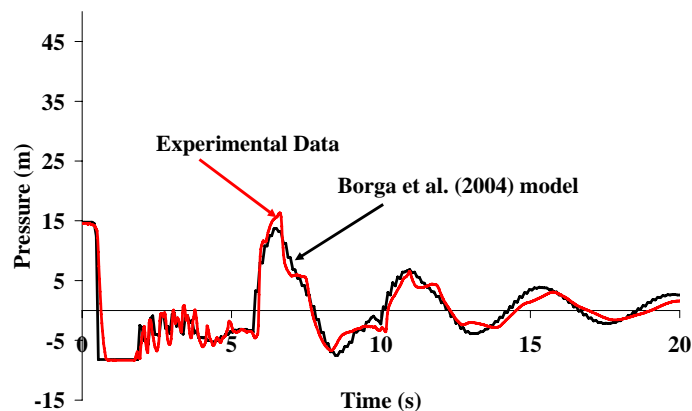


Fig. 9 Borga *et al.*'s model numerical results versus experimental data at Section 5 ( $Q_0 = 4.0$  L/s;  $Re \approx 120,000$ )

Whilst numerically less complex than the viscoelastic model this simplified model can provide better results than those obtained by using both DVCM and viscoelastic model. Actually, the viscoelastic mechanical behaviour of the pipe-walls is described by eq. 15 and the energy dissipation during growth and collapsing of gas cavities is reproduced by the multiplicative coefficients of head loss and characteristic equations.

## 5. Conclusions

The current paper presented experimental tests and numerical analyses of water hammer with cavitation in a pressurised single transmission pipeline composed of high-density polyethylene pipes. Pressure data in turbulent conditions were collected during transient events caused by valve closure. A hydraulic transient solver that takes into account pipe-wall viscoelasticity mechanical behaviour has been developed. Such measured data were used to calibrate and verify three developed mathematical models to the description of cavitating pipe flow: discrete vapour cavity model (DVCM), discrete gas cavity model (DGCM) and a simplified model proposed by Borga *et al.* [18].

Obtained numerical results showed that DVCM is imprecise for the description of hydraulic system behaviour. Whilst such model is on the safest side for design purposes as it predicts higher overpressures, it is not accurate for calibration purposes due to the neglecting of the energy dissipation during the expansion and contraction of the gas cavities. The assumption of the ideal gas law (DGCM) is more appropriate than the simple adoption of vapour pressure when pressure reaches vapour pressure (DVCM) and induces more attenuation and dispersion of transient pressures. For cavitating flows, a new set of viscoelastic parameters was determined and it was assumed that unsteady friction losses, pipe-wall viscoelasticity and wave speed variation due to the formation of localised gas cavities were described by the creep function.

The simplified model proposed by Borga *et al.* [18] provided better results than those obtained by using DVCM. This model can be an alternative numerically less complex than the viscoelastic model.

Considering the analysis carried out in this work, cavitation flows in pressurised systems composed of plastic pipes have to be better analyzed. The study of new numerical methods, such as two-dimensional (2D) methods, can be the solution for the description of pressure transients during cavitation.

## Acknowledgments

The authors gratefully acknowledge the financial support of: “Coordenação de Aperfeiçoamento de Pessoal de Nível Superior” [(CAPES, Brazil), who provided a post-doctoral scholarship to the first author]; the Portuguese Foundation for Science and Technology [(FCT) for grants reference POCTI/ECM/58375/2004, PTDC/ECM/65731/2006, PTDC/ECM/64821/2006, FP7 HYLOW-212423, and for the post-doctoral scholarship provided to the first author (SFRH/BPD/34018/2006)]; CEHIDRO Hydrosystems Research Centre from DECivil/IST; and “Gabinete de Relações Internacionais da Ciência e do Ensino Superior” (GRICES, Portugal).

## Nomenclature

$A$	Pipe cross-sectional area [m <sup>2</sup> ]	$KQ$	Reduction coefficient in the discharge
$a$	Wave speed [m/s]	$N_{KV}$	Number of Kelvin-Voigt elements
$CT$	Parameter which affects the wave speed time variation	$p$	Pressure [Pa]
$D$	Pipe inner diameter [m]	$Q$	Flow rate [m <sup>3</sup> /s]
$e$	Pipe-wall thickness [m]	$t t'$	Time [s]
$E_0$	Young's modulus of elasticity of the pipe [Pa]	$x$	Coordinate along the pipe axis [m]
$E_k$	Modulus of elasticity of the spring of $k$ -element [Pa]	$z$	Elevation of the pipe [m]
$f$	Darcy-Weisbach friction factor	$\alpha$	Dimensionless parameter (function of pipe cross-section dimensions and constraints)
$g$	Gravity acceleration [m/s <sup>2</sup> ]	$\alpha_g$	Gas void fraction
$H$	Piezometric head [m]	$\gamma$	Fluid volumetric weight [N/m <sup>3</sup> ]
$H_v$	Gauge vapour pressure head of the liquid [m]	$\varepsilon_r$	Retarded strain component [m/m]
$h_f$	Head loss per unit length	$\mu_k$	Viscosity of the dashpot of $k$ -element [kg/s.m]
$I$	Head loss term	$\rho$	Liquid mass density [kg/m <sup>3</sup> ]
$J_0$	Creep compliance of the first spring [Pa <sup>-1</sup> ]	$\tau_k$	Retardation time of the dashpot of $k$ -element [s]
$J_k$	Creep compliance of the spring of $k$ -element [Pa <sup>-1</sup> ]	$\psi$	Numerical weighting factor
$KH$	Reduction coefficient in the head variation	$\nabla$	Air cavity volume [m <sup>3</sup> ]
$Re$	Reynolds number ( $=Q_0 D / A v$ )		

## References

- [1] Almeida, A. B. and Koelle, E., 1992, Fluid Transients in Pipe Networks, Computational Mechanics Publications, Elsevier Applied Science, Southampton, UK.
- [2] Wylie, E. B. and Streeter, V. L., 1993, Fluid Transients in Systems, Prentice Hall, Englewood Cliffs, N.J.
- [3] Chaudhry, M. H., 1987, Applied Hydraulic Transients, Litton Educational Publishing Inc., Van Nostrand Reinhold Co, New York, USA.
- [4] Zielke, W., 1968, "Frequency-dependent friction in transient pipe flow," Journal of Basic Engineering, Trans. ASME, Series D, Vol. 90, No. 1, pp. 109-115.
- [5] Covas, D., Ramos, H., Graham, N., and Maksimovic, C., 2005, "Application of hydraulic transients for leak detection in water



supply systems," *Water Science and Technology: Water Supply*, Vol. 4, No. 5-6, pp. 365-374.

[6] Covas, D., Stoianov, I., Mano, J., Ramos, H., Graham, N., and Maksimovic, C., 2004, "The Dynamic Effect of Pipe-Wall Viscoelasticity in Hydraulic Transients. Part I - Experimental Analysis and Creep Characterization," *Journal of Hydraulic Research, IAHR*, Vol. 42, No. 5, pp. 516-530.

[7] Covas, D., Stoianov, I., Mano, J., Ramos, H., Graham, N., and Maksimovic, C., 2005, "The Dynamic Effect of Pipe-Wall Viscoelasticity in Hydraulic Transients. Part II - Model Development, Calibration and Verification," *Journal of Hydraulic Research, IAHR*, Vol. 43, No. 1, pp. 56-70.

[8] Ramos, H., Borga, A., Covas, D., and Loureiro, D., 2004, "Surge damping analysis in pipe systems: modelling and experiments," *Journal of Hydraulic Research, IAHR*, Vol. 42, No. 4, pp. 413-425.

[9] Martin, C. S., 1976, "Entrapped Air in Pipelines," *Proc. 2<sup>nd</sup> Int. Conf. on Pressure Surges, BHRA*, F2.15-F2.27.

[10] Pearsall, I. S., 1965, "The Velocity of the Water Hammer Waves," *Proc. of the Institution of Mechanical Engineers, Symposium on Pressure Surges 1965-66*, pp. 12-20.

[11] Covas, D., Stoianov, I., Ramos, H., Graham, N., and Maksimovic, C., 2003, "The Dissipation of Pressure Surges in Water Pipeline Systems," *Pumps, Electromechanical Devices and Systems Applied to Urban Management, Vol. 2, The Netherlands, Balkema Publishers*, pp. 711-719.

[12] Aklonis, J. J. and MacKnight, W. J., 1983, *Introduction to Polymer Viscoelasticity*, John Wiley & Sons, New York, USA.

[13] Soares, A. K., Covas, D. I. C., and Reis, L. F. R., 2008, "Analysis of PVC Pipe-Wall Viscoelasticity during Water Hammer," *Journal of Hydraulic Engineering, ASCE*, Vol. 134, No. 9, pp. 1389-1394.

[14] Bergant, A., Simpson, A. R., and Tijsseling, A., 2006, "Water Hammer with Column Separation: A Historical Review," *Journal of Fluids and Structures*, Vol. 22, pp. 135-171.

[15] Shu, J. J., 2003, "Modelling Vaporous Cavitation on Fluid Transients," *International Journal of Pressure Vessels and Piping*, Vol. 80, pp. 187-195.

[16] Simpson, A. R. and Bergant, A., 1994, "Numerical comparison of pipe-column-separation models," *Journal of Hydraulic Engineering, ASCE*, Vol. 120, No. 3, pp. 361-377.

[17] Wylie, E. B., 1984, "Simulation of vaporous and gaseous cavitation," *Journal of Fluids Engineering, ASME*, Vol. 106, No. 3, pp. 307-311.

[18] Borga, A., Ramos, H., Covas, D., Dudlik, A., and Neuhaus, T., 2004, "Dynamic effects of transient flows with cavitation in pipe systems," *The Practical Application of Surge Analysis for Design and Operation - 9<sup>th</sup> International Conference on Pressure Surges, Vol. 2, BHR Group Ltd., Bedfordshire, UK*, pp. 605-617.

[19] Carriço, N. G., 2008, "Modelling and Experimental Analysis of Non-Conventional Dynamic Effects during Hydraulic Transients in Pressurised Systems," *Master Thesis, Instituto Superior Técnico, Technical University of Lisbon, Portugal*.